ISSN 2411-3336; e-ISSN 2541-9404

JOURNAL OF MINING INSTITUTE

Zapiski Gornogo instituta

Journal homepage: pmi.spmi.ru

Research article

Geotechnical Engineering and Engineering Geology

High-strength porous ceramics from fine fly ash microspheres

Aleksei V. Ponaryadov✉, Olga B. Kotova, Dmitrii A. Shushkov

Institute of Geology FRC Komi SC UB RAS, Syktyvkar, Komi Republic, Russia

***How to cite this article*:** Ponaryadov A.V., Kotova O.B., Shushkov D.A. High-strength porous ceramics from fine fly ash microspheres. Journal of Mining Institute. 2026. Vol. 281. Iss. 2, p. 80-89.

Abstract

Fly ash can be considered a promising secondary raw material for the production of high-strength porous mullite ceramics, since the absence of a need to grind the initial batch materials makes it possible to significantly reduce energy consumption. In this study, promising ceramic samples were produced using fly ash and aluminum ore, specifically low-iron bauxite, as an Al_2O_3-adjusting component. Thermogravimetric and X-ray diffraction phase analyses were used to determine the sequence and temperature ranges of phase transformations in the system "fly ash – bauxite" and to establish the optimal thermal treatment regime. Several exothermic peaks were observed in the 1200-1300 °C temperature range, reflecting a sequence of phase transformations. Mullite forms through a reaction between quartz and cristobalite, which pass into a transient liquid phase, and γ-Al_2O_3, formed by the decomposition of boehmite. The total mullite phase content reaches 83-84 %, which is significantly higher than the values reported by other researchers, including those who used various additives to accelerate mullite formation. Scanning electron microscopy was used to trace the evolution of the microstructure of the obtained samples as a function of synthesis temperature. As the treatment temperature increases to 1300 °C, sintering gradually intensifies, resulting in the formation of larger pores. Acicular mullite crystals form around flake-like γ-Al_2O_3 crystals, some of which subsequently transform into corundum. Laboratory tests of the finished ceramic samples confirmed that their technical characteristics – density, porosity, and compressive strength – meet the requirements for refractory, thermal insulation, and chemically resistant materials. The study presents the technological principles for developing high-strength and porous mullite-based ceramics intended for use in construction and thermal insulation applications.

Keywords

ceramics; mullite; secondary raw material; fly ash; bauxite; phase transformations

Funding

This work was carried out within the framework of State assignment project N 122040600011-5 at the Institute of Geology FRC Komi SC UB RAS, using the equipment of the CFC "Geoscience" and "Chemistry".

Received: 08.04.2026 ***Accepted: 22.07.2026*** ***Online: 27.10.2026*** ***Published: 30.10.2026***

Introduction

Coal-fired power generation in the Russian Federation annually generates large volumes of ash-and-slag waste (ASW), which poses a threat to the environment. The environmental problems associated with thermal power plant (TPP) waste, including fly ash, are related to its generation, storage, and impact on the environment. According to various estimates, the volume of ASW generated by coal combustion at Russian TPP varies [1, 2]. For example, according to the Ministry of Natural Resources and Environment, more than 22 million tonnes of ASW are generated annually at coal-fired TPP. The total volume of ASW accumulated in ash-and-slag disposal sites at all coal-fired TPP in the country (more than 170 in total, excluding solid-fuel heating boilers) exceeds 1.5 billion tonnes*. The accumulation of large volumes of TPP waste without modern recycling technologies

* Ibragimov E. Ash and Slag from Thermal Power Plants: A Promising Secondary Raw Material. *Energy and Industry of Russia*. 2021. N 13-14 (417-418). URL: https://www.eprussia.ru/epr/417-418/4896283.htm (accessed 23.06.2026).

This is an open access article under the CC BY 4.0 license

creates significant risks for the sustainable development of regions, attracting the attention of specialists in the field of ash waste utilization. One important approach to addressing this problem is the development of effective technologies for using fly ash to produce materials for specific applications, such as the recovery of valuable components [3-5] or the manufacture of new materials [6-8], thereby increasing waste utilization.

Ceramics, including mullite, cordierite, and mullite-anorthite ceramics, belong to the class of high-temperature aluminosilicate materials characterized by a combination of a low coefficient of thermal expansion, low thermal conductivity, and high thermal and chemical resistance in oxidizing and weakly reducing environments. These properties account for their widespread use in the production of refractories, power engineering, and other industries [9-11]. The demand for porous ceramic materials is growing worldwide owing to the implementation of "clean technologies" [12, 13]. For example, the automotive sector is one of the largest consumers of ceramic catalyst supports, driven by the transition to the production of low-emission vehicles and electric vehicles [14]. Industries such as power generation, oil refining, and chemical production use ceramic supports to reduce carbon dioxide emissions [15, 16]. The increased demand for mullite ceramics is accompanied by the need to reduce their production cost and raw-material intensity, which stimulates the search for new sources of aluminum and silicon oxides, such as fly ash [9, 17].

Bauxite and its processed products are traditional sources of aluminum oxide, an Al_2O_3 – adjusting component used in the preparation of initial mixtures for ceramic synthesis. Several studies have demonstrated the possibility of producing low- and medium-porosity mullite and mullite-anorthite ceramics from fly ash-bauxite mixtures with compressive and flexural strength sufficient for their use in construction and refractory applications. The combined use of fly ash and bauxites makes it possible to simultaneously address resource conservation and the utilization of technogenic waste, as well as to control the molar Al_2O_3/SiO_2 ratio in the batch, which determines the intensity of mullitization, pore formation, and the development of the glassy phase [18, 19].

The addition of bauxite to fly ash-based batches promotes the formation of prismatic mullite crystals at relatively low sintering temperatures and enables the production of porous ceramic supports for membranes and filters with satisfactory mechanical properties [20]. The mechanisms by which the phase composition, particle-size distribution, and chemical characteristics of fly ashes and bauxites affect mullite phase formation and the development of an aluminosilicate matrix with a set of performance properties remain insufficiently studied [21, 22].

A relevant task is the development of resource-saving technological approaches to producing mullite-based ceramics from fly ash and bauxite, aimed at expanding the raw-material base of ceramic production and reducing the technogenic impact on the environment. However, the variability of the chemical composition of bauxites limits their use for producing ceramic materials. Therefore, it is relevant to conduct research on the development of physicochemical and technological foundations for obtaining ceramics with predictable and stable properties based on fly ash and low-iron bauxites. These tasks require studying the mineral and particle-size compositions of the initial components, their ratios in the batch, and the effect of heat-treatment parameters on mullite formation, the development of a porous structure, and the mechanical properties of the material. The relevance of producing promising ceramic samples using low-iron bauxites as an Al_2O_3-adjusting component is associated with the fact that low-iron high-modulus bauxites initially contain the required components in permissible amounts, which makes it possible to exclude the stage of producing pure alumina from the alumina ceramic synthesis process.

This study aims to develop the physicochemical and technological basis for producing porous ceramics with predictable and stable properties from fly ash and low-iron bauxites, the latter serving as an Al_2O_3-adjusting component.

This is an open access article under the CC BY 4.0 license

Journal of Mining Institute. 2026. Vol. 281. Iss. 2. P. 80-89
© Aleksei V. Ponaryadov, Olga B. Kotova, Dmitrii A. Shushkov, 2026

Materials and methods

The study was carried out on fly ash samples from the Novo-Irkutskaya (Nis) and Irkutsk-2 (Irk) TPP; chemical compositions are presented in Table 1. The organic carbon content in both samples is insignificant, being less than 0.55 %. The main mineral phases in the fly ash are quartz and mullite. The quartz content in the Irk sample is slightly higher than in Nis (75 and 60 wt.%). Magnetite, hematite, and anhydrite were detected in minor amounts. In addition, an amorphous silicate glassy phase was identified in both fly ash samples, appearing as a broad reflection at 20-30° 2θ. An analysis of the particle-size distribution data showed that the Nis fly ash consists of finer material than the Irk fly ash. More than 82 % of the Nis fly ash material is finer than 0.1 mm, and more than 99 % is finer than 0.25 mm. The proportion of Irk fly ash finer than 0.25 mm is 72 %.

Table 1

Chemical composition of initial materials, wt.%

Sample	Al_2O_3	SiO_2	Fe_2O_3	TiO_2	CaO	MgO	SO_3	Others*
Bauxite	63.50	26.29	3.47	5.05	0.12	–	0.02	1.55
Nis	21.37	61.49	8.41	0.63	5.43	0.81	0.97	0.89
Irk	20.06	56.60	8.12	0.51	9.78	1.28	2.80	0.85

* $Na_2O + K_2O + Mn_2O_3$ + REE.

The Al_2O_3-adjusting component was represented by low-iron bauxite samples from the Vezhay-Vorykvinskoye deposit (Komi Republic, Russia), ground to a fraction finer than 0.01 mm. The bauxite consists of boehmite (41 wt.%), kaolinite (55 wt.%), and rutile (3 wt.%).

The bauxite sample, represented by finely dispersed boehmite particles, contains mechanical inclusions of hematite and rutile up to 10 μm in size (Fig.1, *a*). The fly ash consists of flake-like mullite particles of variable composition with hematite and quartz inclusions (Fig.1, *b*, *c*). Particles with a nearly spherical shape – calcium microspheres – are also present, with a CaO content of up to 24 wt.%. The average microsphere size is (9.8±1.5) μm in the Nis sample and (10.9±1.9) μm in the Irk sample.

The fly ash-to-bauxite ratio was calculated based on the reactions of mullite formation. Since the chemical composition of mullite is variable and can range from $3Al_2O_3 \cdot 2SiO_2$ (3:2) to $2Al_2O_3 \cdot SiO_2$ (2:1), the component ratios were calculated using two reactions. The resulting mixtures and samples were designated 32 and 21, respectively:

$$6\gamma\text{-AlOOH} + 2SiO_2 \rightarrow 3Al_2O_3 \cdot 2SiO_2 + 3H_2O;$$

$$4\gamma\text{-AlOOH} + SiO_2 \rightarrow 2Al_2O_3 \cdot SiO_2 + 2H_2O.$$

The mass of bauxite per 1 g of fly ash was 3.52 g for sample Nis32, 4.70 g for Nis21, 4.41 g for Irk32, and 5.87 g for Irk21.

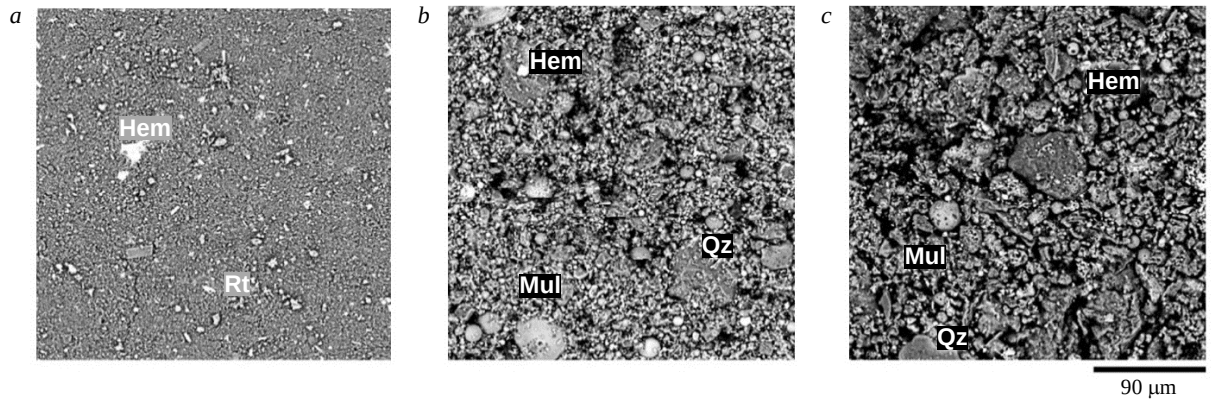


Fig.1. SEM images of low-iron bauxite samples (*a*) and fly ash samples from Nis (*b*) and Irk (*c*). Backscattered electron mode

Hem – hematite; Qz – quartz; Mul – mullite; Rt – rutile

This is an open access article under the CC BY 4.0 license

The reaction mixtures were ground in an agate mortar. A 0.4 g portion of each reaction mixture was formed into disks 10 mm in diameter and 3.2 mm thick by dry pressing (without plasticizers) under uniaxial loading using a manual Carver hydraulic press at a pressure of 45 MPa and a holding time under load of 1 min.

The samples were heat-treated at 1100-1300 °C in alumina crucibles in a Carbolite Gero TF1 16/60/300 tube furnace under an air atmosphere, at a heating rate of 10 °C/min and a holding time of 2 h. After synthesis, the samples were cooled in the furnace to room temperature. The morphology of the initial materials and the resulting ceramic samples was examined by optical microscopy (ADF U300, in transmitted and reflected light) and scanning electron microscopy (KYKY EM-6900 equipped with an X-MAX 50 mm^2 energy-dispersive spectrometer). The phase composition of the samples was determined from X-ray diffraction patterns of unoriented samples. The measurements were performed on a Haoyuan DX-2700BH X-ray diffractometer using CuKα radiation, a Ni filter, an operating power of 40 kV, a current of 30 mA, an SDD detector, and a scanning range of 2-65° 2θ. The phase contents were determined using the Profex software; the content of the X-ray amorphous phase was estimated using an internal standard of 6.5 wt.% zincite. The chemical composition was determined by X-ray fluorescence analysis using a Clever A-17 spectrometer. The phase and chemical compositions were determined once; sample preparation included grinding in an agate mortar to a particle size of less than 0.05 mm. Thermogravimetric analysis was performed using a Netzsch STA 449F5 TGA/DSC instrument over a temperature range of 30-1500 °C at a heating rate of 10 °C/min.

The apparent density, open porosity, and water absorption were determined in accordance with State standard GOST 2409-2014. The mass of the dried sample m_{dry} was measured after drying at 110 °C, with the mass checked every hour. A sample was considered dry if its mass differed from the previous value by no more than 0.1 %. The mass of the water-saturated sample weighed while immersed in distilled water m_{hydr} was determined on an AND GX-400 analytical balance equipped with a hydrostatic weighing device, with the wetted sample fully immersed in the saturating liquid (absolute mass measurement error of 0.01 g). The temperature of the saturating liquid was measured at the same time. The wetted sample was then removed from the vessel, excess liquid was removed from its surface with a damp sponge, and the mass of the saturated sample m_{sat} was determined.

The following equations were used for the calculations:

• apparent density

$$\rho = \frac{m_{dry}}{m_{sat} - m_{hydr}} \rho_w;$$

• open porosity

$$P = \frac{m_{sat} - m_{dry}}{m_{sat} - m_{hydr}} \cdot 100\ \%;$$

• water absorption

$$W = \frac{m_{sat} - m_{dry}}{m_{dry}} \frac{\rho_w^{20}}{\rho_w} \cdot 100\ \%,$$

where ρ_w, ρ_w^{20} – densities of distilled water at the measurement temperature and at 20 °C, respectively.

The compressive strength was determined in accordance with ISO 20504:2006 using an MIM.2-50 automatic testing press. The pressed samples were loaded uniaxially at a rate of 0.05 kN/s until failure; the maximum permissible relative error of force measurement was 0.5 %. The technical properties were measured once.

Results discussion

The appearance of the pressed reaction mixtures and the dense ceramic samples prepared from them is shown in Fig.2. An increase in temperature leads to a significant change in the macroscopic textural characteristics: contact zones become visible, resulting from the physicochemical interaction between fly ash and bauxite during heat treatment.

This is an open access article under the CC BY 4.0 license

Journal of Mining Institute. 2026. Vol. 281. Iss. 2. P. 80-89
© Aleksei V. Ponaryadov, Olga B. Kotova, Dmitrii A. Shushkov, 2026

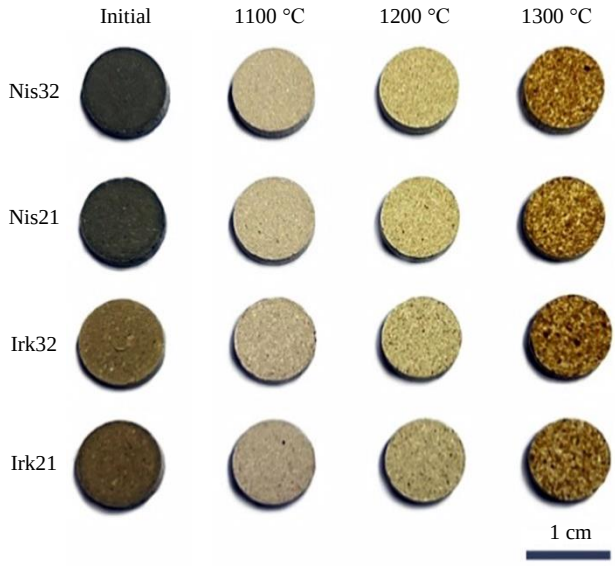


Fig.2. Initial reaction mixtures and the resulting ceramic samples heat-treated at different temperatures

The chemical composition of the resulting ceramic samples is presented in Table 2. For all the reaction mixtures studied, the Al_2O_3-to-SiO_2 content ratio changes with increasing heat-treatment temperature, which indirectly indicates the formation of new mineral phases in the system and changes in the morphostructural characteristics of the ceramics. The CaO impurity present in the system can act as a mineralizer, increasing the rate of mullite formation and lowering the sintering temperature by 70-150 °C through the formation of eutectics [23, 24].

The phase composition of the resulting ceramic samples (Fig.3) is represented by the following major phases: mullite, cristobalite, quartz, corundum, and γ-Al_2O_3. Weak reflections of rutile and hematite were also detected. With increasing heat-treatment temperature, the crystallinity of the material increases. The intensities of the reflections of cristobalite (d/n ≈ 4.10, 3.22, and 2.50 Å), quartz (d/n ≈ 4.28, 3.37, and 2.13 Å), corundum (d/n ≈ 3.49, 2.38, and 2.09 Å), and γ-Al_2O_3 (d/n ≈ 2.81 and 1.96 Å) also decrease. Cristobalite and quartz are not detected in the samples obtained at 1300 °C. At the same time, corundum partially remains, which may be associated with the presence of aluminum in kaolinite, whose content was not taken into account in the component calculations. Simultaneously, the intensity of the mullite reflections increases; these reflections are somewhat broadened owing to the overlap of the mullite-32 and mullite-21 phases, which is clearly visible in the {210} reflection (d/n ≈ 3.39 and 3.43 Å, respectively). For the Irk32 sample synthesized at 1100 °C, a small region of elevated background is observed in the 20-30° 2θ range, which may be associated with the presence of an X-ray amorphous glassy phase (~30 %) in the sample.

Table 2

Chemical composition of the ceramic samples, wt.%

Sample	*T*, °C	Al_2O_3	SiO_2	Fe_2O_3	TiO_2	CaO	Others*
Nis32	1100	61.61	27.50	4.80	3.97	1.49	0.63
	1200	59.30	29.64	4.89	4.06	1.52	0.59
	1300	55.16	32.16	5.82	4.54	1.63	0.69
Nis21	1100	59.91	30.09	4.22	3.96	1.21	0.61
	1200	57.85	31.35	4.70	4.21	1.30	0.59
	1300	55.38	33.22	5.06	4.44	1.26	0.64
Irk32	1100	59.79	29.12	4.36	4.07	2.09	0.57
	1200	56.55	32.01	4.51	4.18	2.19	0.56
	1300	53.49	34.48	4.86	4.48	2.09	0.60
Irk21	1100	62.33	27.60	3.87	4.07	1.56	0.57
	1200	59.58	29.78	4.12	4.29	1.68	0.55
	1300	56.36	31.99	4.64	4.79	1.62	0.60

* Na_2O + K_2O + Mn_2O_3 + REE.

An analysis of the phase contents determined by the Rietveld method (Table 3) shows that the mass fractions of the corundum and γ-Al_2O_3 phases are inversely related to that of mullite. For the samples obtained at 1100 °C, the total mullite content (~25-27 %) correlates with that in the initial fly ash. Taking into account the presence of γ-Al_2O_3 in the system, it can be concluded that mullite formation is not possible at this temperature. An increase in temperature leads to a solid-state reaction

This is an open access article under the CC BY 4.0 license

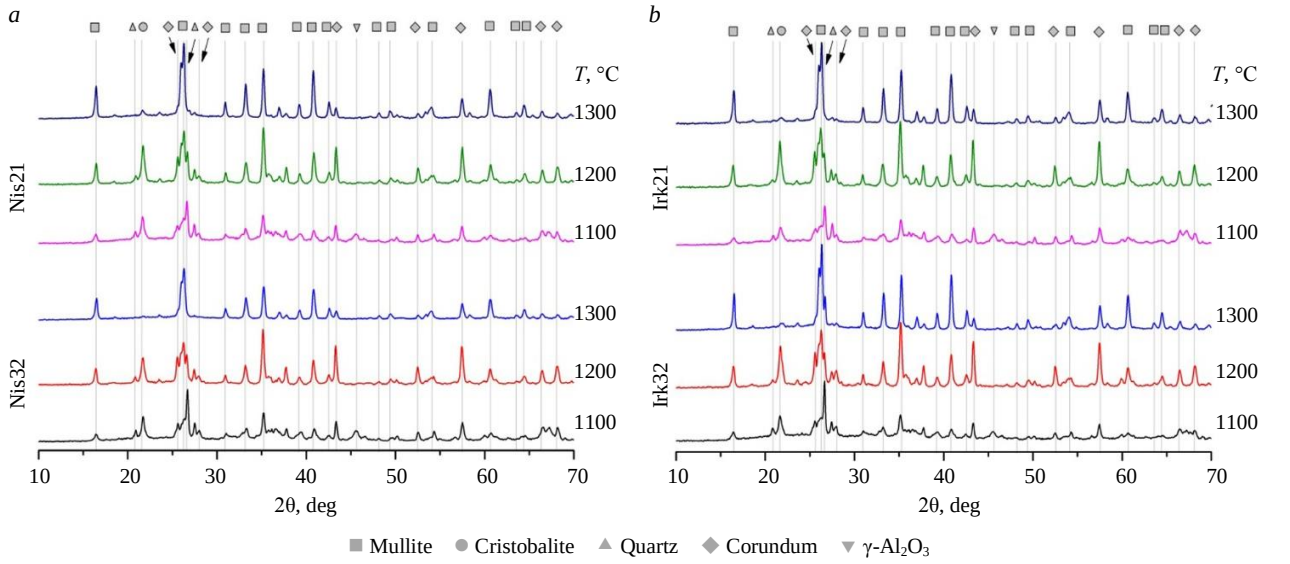


Fig.3. X-ray diffraction patterns of the Nis (*a*) and Irk (*b*) ceramic samples obtained at different temperatures

Table 3

Phase composition of the ceramic samples, wt.%

Sample	*T*, °C	γ-Al_2O_3	Corundum	Mullite-21	Mullite-32	Quartz	Cristobalite	Rutile	Hematite
Nis32	1100	25	20	5	20	12	13	3	2
	1200	0	36	5	41	6	8	2	2
	1300	0	12	25	59	1	1	1	1
Nis21	1100	24	18	6	22	12	12	4	2
	1200	0	28	2	51	6	10	2	1
	1300	0	11	25	60	1	1	1	1
Irk32	1100	17	17	4	11	6	10	3	2
	1200	0	31	3	43	5	13	2	2
	1300	0	10	0	83	4	1	2	1
Irk21	1100	28	18	8	19	9	13	3	2
	1200	0	31	2	46	6	11	2	2
	1300	0	13	25	58	1	1	1	1

between quartz, cristobalite, and the polymorphic modifications of Al_2O_3 (γ-Al_2O_3 and corundum). As a result, mullite forms with a further increase in temperature, while an excess of corundum remains in the system [25, 26]. An analysis of the SiO_2-Al_2O_3 phase diagram shows that the stability region of the mullite-32 phase is small. Given that mullite is characterized by heterovalent isomorphous substitution, $2Si^{4+} + O^{2-} \rightarrow 2Al^{3+} + \square$, where □ denotes an oxygen vacancy [23], an increase in the treatment temperature will lead not only to mullite formation but also to a phase transition with the formation of intermediate incommensurate phases. This explains the increase in the proportion of the mullite-21 phase, which can form solid solutions with corundum. The total mullite phase content increases to 83-84 %. This is significantly higher than the values reported by other researchers, including those who used additives to accelerate mullite formation [27-29]. In this study, in addition to the CaO impurity in the initial fly ash samples, rutile inclusions may also have had a positive effect. L.Mahnicka-Goremikina et al. [30] noted that micro- and especially nano-sized TiO_2 additives act as sintering activators and crystallization centers; small amounts (1-5 wt.%) noticeably accelerate mullite formation and make it possible to achieve a higher degree of conversion of the batch components into mullite at the same sintering temperature.

On the thermogravimetric (TG) curves of all the ceramic samples studied, mass loss occurs in the 490-560 °C range and is associated with the removal of constitutional water from boehmite and

This is an open access article under the CC BY 4.0 license

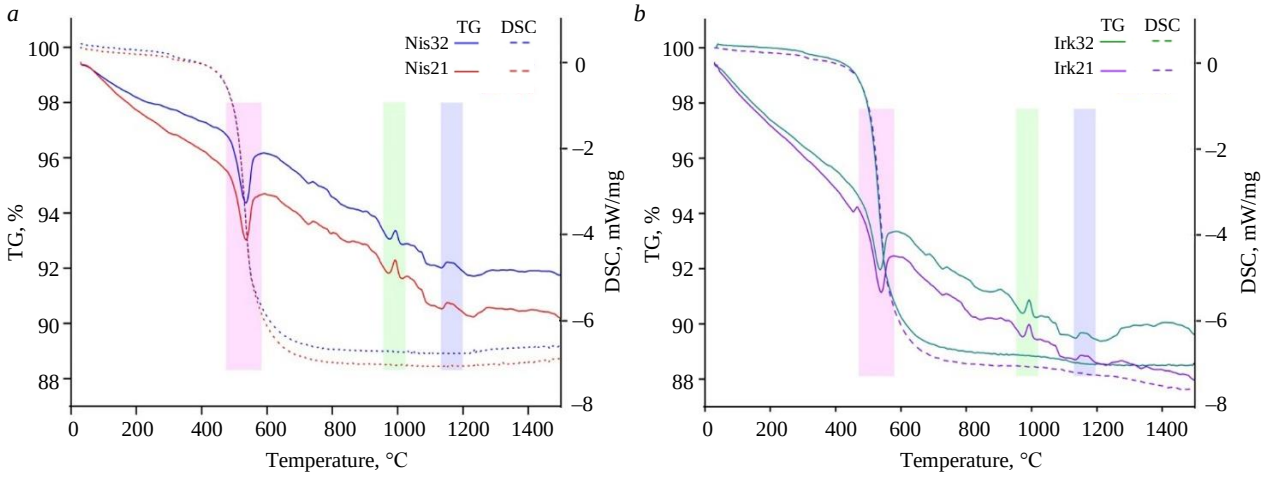


Fig.4. TG and DSC curves of the Nis (*a*) and Irk (*b*) ceramic samples

the formation of γ-Al_2O_3 (Fig.4). The first exothermic peak in the 975-1010 °C range is associated with the final destruction of the crystal structure of kaolinite contained in the bauxite, namely the decomposition of metakaolinite into free oxides, the breaking of bonds between silicon-oxygen tetrahedra, a partial increase in the coordination number of aluminum ions, and the formation of cristobalite [26, 31]. With a further increase in temperature, several exothermic peaks with diffuse boundaries are observed on the differential scanning calorimetry (DSC) curves, reflecting the sequence of phase transformations described above.

The morphostructural features of the resulting ceramic samples were examined by optical microscopy (Fig.5). Mechanical impurities of rutile and hematite were identified in the initial mixtures and persisted after heat treatment at 1100 and 1200 °C. Rutile occurs as elongated prismatic crystals of reddish-brown and yellow-brown color, with striations clearly visible on the faces parallel to the axis. Hematite forms black granular aggregates and appears gray-blue in reflected light. The resulting corundum occurs as yellow columnar crystals and is distinguished by high relief. With increasing temperature, an ochre-colored mullite matrix begins to appear in all samples. The ceramic samples obtained at 1200 and 1300 °C are characterized by the appearance of macropores up to 10 μm in size. As the temperature rises, foreign ions are incorporated into the mullite crystal lattice to a greater degree. Fe^{3+} cations can form solid solutions based on mullite by substituting for aluminum in octahedral sites [23]. Hematite is not detected in the ceramic samples obtained at 1300 °C.

The evolution of the microstructure of the resulting ceramic samples is shown in Fig.6. At 1100 °C, a porous structure forms as a result of partial sintering of the mixture of fly ash and bauxite particles. The pore size does not exceed a few micrometers. Mechanical inclusions of quartz, hematite, and rutile, as well as flake-like γ-Al_2O_3 crystals, are present on the surface. In the 1200-1300 °C range, sintering gradually intensifies, producing larger pores. Thin needle-like mullite crystals presumably form around the flake-like γ-Al_2O_3 crystals, some of which transform into corundum. The amorphous glassy phase noted in [32] is not detected in the samples studied. As the treatment temperature rises, the Al_2O_3/SiO_2 ratio in the matrix decreases, which is associated with the formation of the mullite-32 phase and the development of a more homogeneous porous microstructure. When the sintering temperature reaches 1300 °C, the samples become denser, which will affect their open porosity. The appearance of larger pores at higher synthesis temperatures may be related to volume expansion resulting from the growth of elongated prismatic mullite crystals [33, 34].

This is an open access article under the CC BY 4.0 license

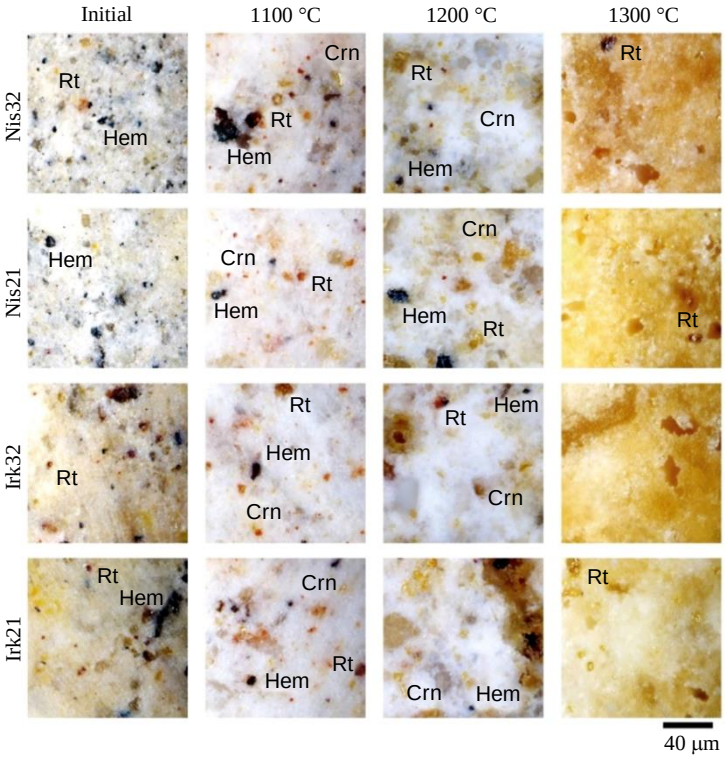


Fig.5. Morphostructural features of the resulting ceramic samples
Crn – corundum

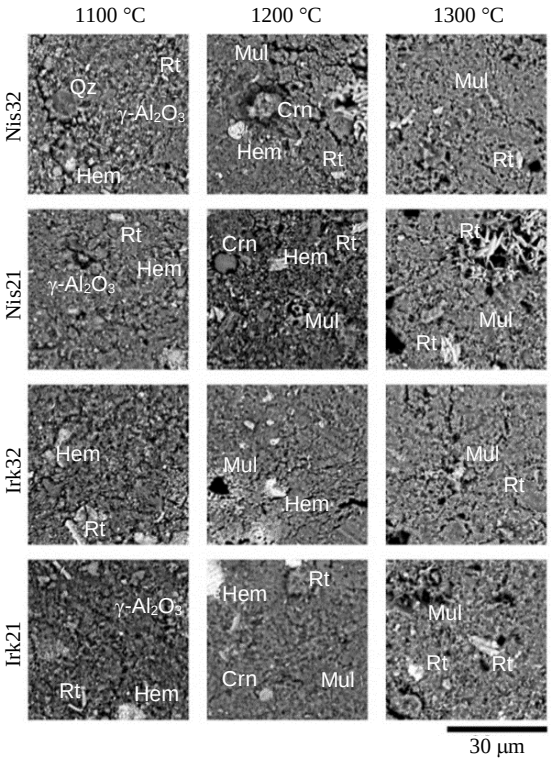


Fig.6. SEM images of the ceramic samples.
Backscattered electron mode

The technical characteristics of the resulting ceramic samples are presented in Table 4. As the temperature rises, the density of the samples grows markedly: porosity falls while density climbs. For the samples obtained at 1100 °C, the high open porosity values are due to the decomposition of boehmite, whose structure releases hydroxyl groups on heating, which can lead to the formation of a large number of micropores. At higher treatment temperatures, porosity declines despite the formation of macropores, and the density of the ceramic samples rises in parallel. The sintering and densification of the samples are influenced by polymorphic transformations (for example, γ-Al_2O_3 → → corundum) [35]. On the other hand, impurities such as CaO act as modifiers of glassy phase formation and lower the temperature at which quartz and cristobalite begin to react with Al_2O_3.

Table 4

Technical properties of the synthesized ceramic samples

Sample	*T*, °C	Apparent density, g/cm^3	Open porosity, %	Water absorption, %	Compressive strength, MPa
Nis32	1100	1.91 ± 0.05	34.73 ± 2.97	18.18 ± 0.57	39 ± 0.2
	1200	2.11 ± 0.06	30.00 ± 4.34	14.20 ± 0.44	78 ± 0.4
	1300	2.17 ± 0.06	21.79 ± 2.41	10.03 ± 0.48	87 ± 0.4
Nis21	1100	2.02 ± 0.06	31.03 ± 4.16	15.34 ± 0.45	45 ± 0.2
	1200	2.19 ± 0.06	27.45 ± 4.27	12.50 ± 0.42	100 ± 0.5
	1300	2.25 ± 0.07	19.74 ± 2.34	8.77 ± 0.37	108 ± 0.5
Irk32	1100	1.98 ± 0.05	32.56 ± 3.27	16.42 ± 0.42	58 ± 0.3
	1200	2.09 ± 0.05	29.88 ± 3.24	14.29 ± 0.42	69 ± 0.3
	1300	2.17 ± 0.06	18.99 ± 2.88	8.72 ± 0.30	70 ± 0.3
Irk21	1100	1.99 ± 0.05	32.02 ± 3.54	16.10 ± 0.26	61 ± 0.3
	1200	2.10 ± 0.06	30.25 ± 2.59	14.37 ± 0.25	106 ± 0.5
	1300	2.22 ± 0.06	20.00 ± 2.37	9.01 ± 0.26	117 ± 0.6

This is an open access article under the CC BY 4.0 license

An analysis of the data in Table 4 shows that the resulting ceramic samples have characteristics – apparent density, porosity, and compressive strength – that meet the requirements for thermal-insulating and chemically resistant materials and refractories, and are comparable to analogues [17, 32].

Conclusion

Fly ash is a finely dispersed aluminosilicate material with a uniform particle-size distribution and serves as a raw material for synthesizing aluminosilicate matrices with low energy consumption, since there is no need to grind the initial batch materials. It can be regarded as a promising secondary raw material for ceramic production.

Ceramic samples were produced using low-iron bauxites as an Al_2O_3-adjusting material. Mullite is the major phase. Based on thermogravimetric and X-ray diffraction phase analysis data, the sequence and temperature ranges of phase transitions in the "fly ash – bauxite" system were determined, and the heat-treatment regime was substantiated.

It was established that, for the samples obtained at 1100 °C, the total mullite content does not exceed 27 %, which correlates with its content in the batch. At the same time, an excess of corundum remains in the system. An increase in the treatment temperature leads to mullite formation through a solid-state reaction between quartz and cristobalite, which pass into a transient liquid phase, and γ-Al_2O_3, formed by the decomposition of boehmite. The crystallinity of the samples rises. An increase in the proportion of the mullite-21 phase is also observed; this phase can form solid solutions with corundum. The total mullite phase content rises to 83-84 %, which is considerably higher than the values reported by other researchers, including those who used additives to accelerate mullite formation.

The resulting ceramics, with the density, porosity, and compressive strength values indicated above, are expected to find applications in various industrial and construction applications, where they can protect equipment, structures, and technological processes from extreme impacts.

The technological principles presented for producing high-strength and, where required, porous mullite ceramics from technogenic raw materials are important for industrially developed regions with a high concentration of thermal power and aluminum production facilities. Such ceramics are intended for construction and thermal insulation applications.

REFERENCES

1. Taskin A.V., Fediuk R.S., Fedotov D.R. Complex processing of ash and slag waste from coal-fired power plants and coal enrichment waste. *Bulletin of the Kuzbass State Technical University.* 2025. N 1 (167), p. 28-36 (in Russian). DOI: 10.26730/1999-4125-2025-1-28-36

2. Kalinkin A.M., Kalinkina E.V., Ivanova A.G., Kruglyak E.A. Geopolymers based on mechanically activated mixtures of coal-fired power plant fly ash with natural calcium and magnesium carbonates. Trudy Fersmanovskoi nauchnoi sessii GI KNT RAN. Apatity: Geologicheskii institut KNTs RAN, 2022. N 19, p. 144-148 (in Russian). DOI: 10.31241/FNS.2022.19.027

3. Hasanuzzaman Md., Quddus Md.S., Saha M., Sharmin N. Transformation of waste into wealth: Thermochemical conversion of coal fly ash to extract Al_2O_3 via alkali desilication and soda – lime assisted sintering. *Chemistry of Inorganic Materials*. 2026. Vol. 8. N 100143. DOI: 10.1016/j.cinorg.2026.100143

4. Mingfei Xing, Xiaofang Wu, Zixin Li et al. Rare earth element recovery and aluminum-rich residue production from high alumina fly ash by alkali pre-desilication enhance the mechanochemical extraction process. *Process Safety and Environmental Protection*. 2023. Vol. 175, p. 60-69. DOI: 10.1016/j.psep.2023.05.022

5. Kumar A., Samadder S.R., Elumalai S.P. Recovery of Trace and Heavy Metals from Coal Combustion Residues for Reuse and Safe Disposal: A Review. *JOM*. 2016. Vol. 68. N 9, p. 2413-2417. DOI: 10.1007/s11837-016-1981-3

6. Delitsyn L.M., Kulumbegov R.V., Popel O.S. et al. Processing of Ash and Slag Waste from Coal-Fired Thermal Power Plants and Extraction of Commercial Products from the Waste (Review). *Thermal Engineering*. 2025. Vol. 72. N 3, p. 203-220. DOI: 10.1134/S0040601524700836

7. Krasnyi B.L., Ikonnikov K.I., Lemeshev D.O., Sizova A.S. Fly Ash as Technogenic Raw Material for Producing Refractory and Insulating Ceramic Materials (Review). *Glass and Ceramics*. 2021. Vol. 78. N 1-2, p. 48-56. DOI: 10.1007/s10717-021-00347-3

8. Kotova O.B., Shabalin I.N., Shushkov D.A., Kocheva L.S. Hydrothermal synthesis of zeolites from coal fly ash. *Advances in Applied Ceramics: Structural, Functional and Bioceramics*. 2016. Vol. 115. Iss. 3, p. 152-157. DOI: 10.1179/1743676115Y.0000000063

9. Yang Luo, Shuhua Ma, Shili Zheng et al. Mullite-based ceramic tiles produced solely from high-alumina fly ash: Preparation and sintering mechanism. *Journal of Alloys and Compounds*. 2018. Vol. 732, p. 828-837. DOI: 10.1016/j.jallcom.2017.09.179

10. Guanghui Li, Qunzhen Bu, Hu Sun et al. Cost-Effective and Sustainable Preparation of Porous Mullite-Based Ceramics Combining MoO_3 Recovery from Industrial Calcine. *ACS Sustainable Chemistry & Engineering*. 2020. Vol. 8. Iss. 19, p. 7290-7299. DOI: 10.1021/acssuschemeng.0c00079

This is an open access article under the CC BY 4.0 license

11. Vakalova T., Sergeev N., Tolegenov D., Tolegenova D. High-strength building ceramics based on fly ash – red mud mixtures. *Magazine of Civil Engineering*. 2023. Vol. 121. Iss. 5. N 12104. DOI: 10.34910/MCE.121.4

12. Babashov V.G., Varrik N.M., Karaseva T.A. Porous ceramic for filtration of metal melts and hot gases (review). *Proceedings of VIAM.* 2020. N 8 (90), p. 54-63 (in Russian). DOI: 10.18577/2307-6046-2020-0-8-54-63

13. Akimochkina G.V., Fomenko E.V., Fadeeva N.P. et al. High Strength Porous Ceramics Based on Disperse Microspheres of Fly Ash and Pearlite. *Journal of Siberian Federal University. Chemistry.* 2024. Vol. 17 (3), p. 339-349 (in Russian).

14. Sassykova L.R., Gilmundinov Sh.A., Massenova A.T. et al. Catalysts on metal and ceramic carriers for neutralization of waste gases of industry and motor transport. *News of the National Academy of Sciences of the Republic of Kazakhstan. Series of chemistry and technology.* 2016. Vol. 3. N 417, p. 135-144 (in Russian).

15. Noskov A.S The scientific and technical level of research and the prospects for import substitution in the field of industrial catalysts. *Vestnik Rossiiskoi akademii nauk.* 2022. Vol. 92. N 10, p. 940-949. DOI: 10.31857/S0869587322100085

16. Mengdan Huo, Tong Yu, Yu Wang et al. In-situ Ti doping induces distortion of mullite whiskers in fly ash-based ceramic membranes for enhanced oil-water separation performance. *Journal of Environmental Chemical Engineering*. 2025. Vol. 13. Iss. 6. № 119281. DOI: 10.1016/j.jece.2025.119281

17. Roy R., Das D., Rout P.K. Mullite Ceramics Derived from Fly Ash Powder by Using Albumin as an Organic Gelling Agent. *Biointerface Research in Applied Chemistry*. 2023. Vol. 13. Iss. 4. N 339. DOI: 10.33263/BRIAC134.339

18. Beiyue Ma, Chang Su, Xinming Ren et al. Preparation and properties of porous mullite ceramics with high-closed porosity and high strength from fly ash via reaction synthesis process. *Journal of Alloys and Compounds*. 2019. Vol. 803, p. 981-991. DOI: 10.1016/j.jallcom.2019.06.272

19. Zhengbo Li, Yuhao Peng, Hongda Ren et al. Co-sintering of bauxite tailings and fly ash for low-density ceramic proppants: Sintering mechanism and process optimization. *Ceramics International*. 2025. Vol. 51. Iss. 26. Part C, p. 51267-51277. DOI: 10.1016/j.ceramint.2025.08.353

20. Yingchao Dong, Hui Wu, Fenglin Yang, Stephen Gray. Cost and efficiency perspectives of ceramic membranes for water treatment. *Water Research*. 2022. Vol. 220. N 118629. DOI: 10.1016/j.watres.2022.118629

21. Wan Fan, Dong Zou, Jingrui Xu et al. Enhanced Performance of Fly Ash-Based Supports for Low-Cost Ceramic Membranes with the Addition of Bauxite. *Membranes*. 2021. Vol. 11. Iss. 9. N 711. DOI: 10.3390/membranes11090711

22. Zou Xinwei, Hou Ruyuan, Hao Jianying et al. The low temperature preparation of ultra low-density ceramic proppants by adding fly ash. *Ceramics-Silikáty*. 2020. Vol. 64. Iss. 2, p. 107-114. DOI: 10.13168/cs.2019.0055

23. Yarotskaya E.G., Fedorov P.P. Mullite and its isomorphic substitution. Overview. *Condensed Matter and Interphases.* 2018. Vol. 20. N 4, p. 537-544 (in Russian). DOI: 10.17308/kcmf.2018.20/626

24. Grushko I.S. Ways of Formation and Features of Development of the Crystal Phase in Amorphous Material (A Review). *Glass Physics and Chemistry.* 2020. Vol. 46. N 6, p. 549-561. DOI: 10.1134/S1087659620060103

25. Koshy P., Ho N., Zhong V. et al. Fly Ash Utilisation in Mullite Fabrication: Development of Novel Percolated Mullite. *Minerals*. 2021. Vol. 11. Iss. 1. N 84. DOI: 10.3390/min11010084

26. Kotova O.B., Ustyugov V.A., Shiyong Sun, Ponaryadov A.V. Mullite production: phase transformations of kaolinite, thermodynamics of the process. *Journal of Mining Institute.* 2022. Vol. 254, p. 129-135. DOI: 10.31897/PMI.2022.43

27. Wei Lian, Yan Liu, Wenjie Wang et al. Preparation of environmentally friendly low-cost mullite porous Ceramics and the effect of Waste Glass Powder on structure and mechanical Properties. *International Journal of Precision Engineering and Manufacturing-Green Technology*. 2022. Vol. 9. Iss. 2, p. 577-585. DOI: 10.1007/s40684-021-00333-8

28. Dey S., Ray D., Mondal A., Parya T.K. Effect of yttria on sintering and microstructural behavior of reaction sintered mullite based on bauxite, fly ash and precipitated silica. *Ceramics International*. 2018. Vol. 44. Iss. 9, p. 10087-10093. DOI: 10.1016/j.ceramint.2018.02.214

29. Mao Fu, Jing Liu, Xinfa Dong et al. Waste recycling of coal fly ash for design of highly porous whisker-structured mullite ceramic membranes. *Journal of the European Ceramic Society*. 2019. Vol. 39. Iss. 16, p. 5320-5331. DOI: 10.1016/j.jeurceramsoc.2019.08.042

30. Mahnicka-Goremikina L., Rundans M., Goremikins V. et al. Effect of Microsize and Nanosize TiO_2 on Porous Mullite-Alumina Ceramic Prepared by Slip Casting. *Materials*. 2024. Vol. 17. Iss. 24. N 6171. DOI: 10.3390/ma17246171

31. Olcoski T.A., Chinelatto A.L., Chinelatto A.S.A. Effect of MgO addition on the sinterability and mechanical properties of mullite ceramics. *Cerâmica*. 2021. Vol. 67 (383), p. 261-268. DOI: 10.1590/0366-69132021673833075

32. Jian-bin Zhu, Hong Yan. Microstructure and properties of mullite-based porous ceramics produced from coal fly ash with added Al_2O_3. *International Journal of Minerals, Metallurgy, and Materials*. 2017. Vol. 24. Iss. 3, p. 309-315. DOI: 10.1007/s12613-017-1409-2

33. Zhiwen Zhu, Zhaoling Wei, Wenping Sun et al. Cost-effective utilization of mineral-based raw materials for preparation of porous mullite ceramic membranes via in-situ reaction method. *Applied Clay Science*. 2016. Vol. 120, p. 135-141. DOI: 10.1016/j.clay.2015.11.020

34. Zhentao Cui, Tianran Hao, Shuaifeng Yao, Hongliang Xu. Preparation of porous mullite ceramic supports from high alumina fly ash. *Journal of Material Cycles and Waste Management*. 2023. Vol. 25. Iss. 2, p. 1120-1129. DOI: 10.1007/s10163-023-01598-8

35. Belyaev I.V., Stepnov A.A., Mogilnikov P.S., Kireev A.V. Effect of Heat Treatment Temperature on Dilatometric and Densimetric Characteristics of Plasma-Sprayed Al_2O_3 Ceramics. *Inorganic Materials.* 2022. Vol. 58. N 7, p. 744-750. DOI: 10.1134/S0020168522070044

***Authors*: Aleksei V. Ponaryadov,** *Junior Researcher* (*Institute of Geology FRC Komi SC UB RAS, Syktyvkar, Komi Republic, Russia*), *avponaryadov@geo.komisc.ru, https://orcid.org/0000-0003-1166-2408*, **Olga B. Kotova,** *Doctor of Geological and Mineralogical Sciences, Chief Researcher* (*Institute of Geology FRC Komi SC UB RAS, Syktyvkar, Komi Republic, Russia*), *https://orcid.org/0000-0001-8448-3385*, **Dmitrii A. Shushkov,** *Candidate of Geological and Mineralogical Sciences, Senior Researcher* (*Institute of Geology FRC Komi SC UB RAS, Syktyvkar, Komi Republic, Russia*), *https://orcid.org/0000-0002-7856-8080*.

The authors declare no conflict of interests.

This is an open access article under the CC BY 4.0 license